Engineering Transactions, **67**(3): 369–386, 2019, doi: 10.24423/EngTrans.939.20190426
Polish Academy of Sciences • Institute of Fundamental Technological Research (IPPT PAN)
Université de Lorraine • Poznan University of Technology

Research Paper

Investigation of Monotonic and Cyclic Behavior of Soft Clay Using Direct Simple Shear Apparatus

Sutera BENCHANUKROM[1)], Chitsirin LAILAK[2)], Nirut KONKONG[3)]

[1)] *Department of Industrial Construction Technology*
Faculty of Agricultural Technology and Industrial Technology
Phetchabun Rajabhat University
Phetchabun, 67000, Thailand

[2)] *Research and Development Institute*
Pibulsongkram Rajabhat University
Phitsanulok 65000, Thailand

[3)] *P.A.I.R Engineering Co., Ltd*
Bangkok, 10210, Thailand
Corresponding Author e-mail: nirut.k@ku.th

The purpose of this research was to study the monotonic and cyclic simple shear mode behavior of Bangkok clay, using direct simple shear apparatus. The monotonic specimens were prepared in a saturated condition and were K_0 consolidated before being undrained sheared. The specimens were sheared at the shear strain rate of 5% per hour until the shear strain reached 20%. The Stress History and Normalized Soil Engineering Properties (SHANSEP) method was applied to analyze the monotonic test data, and the CK_0DSS SHANSEP equation was proposed, based on the results. The results from the CK_0DSS SHANSEP equation were in a good correlation with Q_u, CK_0CU and CK_0EU. The cyclic specimens were tested at different frequencies of 0.1, 1 and 5 Hz and the vertical stress was varied at 200, 300, and 400 kPa. The shear strain amplitude was controlled at $\pm 0.5\%$ for the first 100 cycles, and then was increased to $\pm 1.5\%$ for the next 100 cycles, and finally it was increased to $\pm 3\%$ for the last 100 cycles. The results showed that the shear modulus increased when the maximum vertical effective stress increased and the damping ratio increased when the strain amplitude increased.

Key words: monotonic test; cyclic test; direct simple shear apparatus; SHANSEP; shear modulus; damping ratio.

1. Introduction

Geotechnical engineering problems can be divided into two categories: soil stability and displacement problem. Knowledge of soil failure behavior as well

as soil's deformation and shear strength is essential and it is necessary for simulations of these mechanisms in the laboratory. Geological engineering work may cause slope instability, and consequently a specific device is necessary to simulate slope stability and possible failure. An example of a 2D slope stability problem is illustrated in Fig. 1, showing that the shear strength at the base of a slip surface is best tested as a direct simple shear, the area near the toe is best represented by triaxial extension, and the area at or near the tip is best represented by triaxial compression.

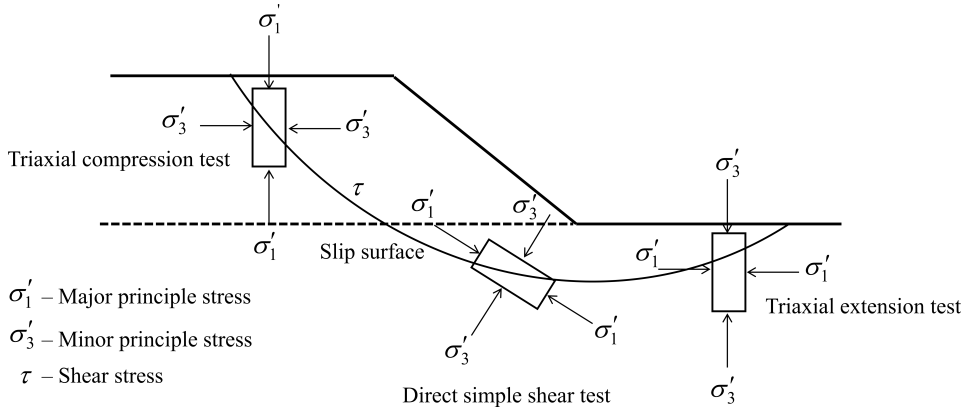

FIG. 1. The failure mechanisms in different zones of the embankment.

The advantage of the direct simple shear test over the triaxial test lies in the fact that in the former test the principal stresses are allowed to rotate during shearing, and the specimen is kept in a plane strain condition [1]. However, the inability to impose uniform normal and shear stress on a specimen is discussed in FINN *et al.* [2], LUCKS *et al.* [3] and PREVOST, HOEG [4]. Normal and shear stress are improved by adjusting the ratio of specimen height and diameter, the percentage of wire-reinforcement and applied horizontal displacement [5]. In other cases, direct simple shear apparatus is used to study the clay behavior due to the cyclic loading, which can be measured as undrained shear strength, excess pore pressure and shear modulus [6–12].

In Thailand, Bangkok clay originates from sedimentation deposited in the delta of the Chao Phraya River. It is described as grey and greenish-grey clay and silt with no mottle. The clay minerals include montmorillonite ≈60%, kaolinite ≈25%, and illite ≈15% [13]. Bangkok clay is characterized by high compressibility, low shear strength and low permeability, while a high settlement rate a major problem that arises after construction and continues over the lifetime of a constructed road embankment. Previous studies have found that the influence of dynamic traffic loading is greater than the embankment static self-weight

loading [14, 15]. Although the Bangkok area is located in a low seismic hazard area, with the active fault zones being located about 185 km to 400 km from the city [16], seismic wave amplification of Bangkok clay must be carefully evaluated before structural design takes place. In practice, the strength properties of Bangkok clay are investigated based on the results of unconfined compression tests, the standard penetration test (SPT), or unconsolidated undrained triaxial testing. Direct simple tests, such as monotonic tests and cyclic tests, are excessively costly, and consequently they are not commonly used test procedures in geotechnical engineering practice in Thailand. Given that, the knowledge about the stress-strain behavior, deformation and shear strength behavior of Bangkok clay in the simple shear mode, needs to be substantially expanded, particularly cyclic simple shear soil parameters should be defined to enable engineers to use them for improved foundation design and construction.

The purpose of this research, therefore, was to study the monotonic and cyclic simple shear mode behavior of Bangkok clay using direct simple shear apparatus, and to determine the monotonic and cyclic soil properties: undrained shear strength, shear modulus and damping ratio of Bangkok clay. Normally consolidated (NC) samples and over-consolidated (OC) samples were subjected to undrained monotonic shearing tests. The SHANSEP technique [17] was used to analyze the monotonic shear loading response, based on which we proposed CK_0DSS SHANSEP parameters for estimating how the undrained shear strength varies with depth. For cyclic shear loading, the normally consolidated samples were subjected to cyclic shearing with a series of two-way strain-controlled tests. Cyclic shear stress (τ), pore water pressure (Δu), shear modulus (G_{avg}) and damping ratio (D_{avg}) measurements were obtained. These are widely known in earthquake engineering as the fundamental parameters describing the dynamics of soil behavior.

2. Material and method

2.1. Bangkok clay

All soil specimens were taken from a borehole, centrally located in the Bangkok area. The borehole was drilled by the wash boring method to a depth of 15.5 m. A 1 m long Shelby tube of a diameter of 7.6 cm was used to obtain a soil specimen at that depth. In the laboratory, the soil specimen was pushed out of the Shelby tube by a hydraulic jack, and a 20 cm undisturbed sample was taken from the center of the core and wrapped in aluminum foil and a paraffin wax coating. The 20 cm portions of the core are called disturbed samples, and these were studied for their basic soil properties, such as moisture content, liquid limit, plastic limit, plasticity index, specific gravity and unit of weight (Table 1).

Table 1. Results of basic soil properties.

Item	Value	Average
Depth [m]	2.5–15.5	
Moisture contents, w [%]	59–62	60.34
Liquid limit, LL [%]	78–83	82.61
Plastic limit, PL [%]	41–44	43.12
Plastic index, PI [%]	37–39	38.32
The specific gravity of solid soils	2.62–2.64	2.63
Unit of weight [kN/m^3]	15.83–16.01	15.90

The stress history of the components of the specimen, including maximum past pressure (σ'_p) and over-consolidation ratio (OCR), were measured by a consolidation test (oedometer test), which included the loading sequences of 1/8, 1/4, 1/2, 1, 2, 4 and 8-times of the overburden pressure (σ'_{v0}), and the unloading pressures at 2 and 0.5-times of the overburden pressure. The results were a maximum past pressure of 130 kPa and the OCR of 1.49, as measured by the oedometer apparatus.

2.2. Direct simple shear apparatus

At Chulalongkorn University, Thailand, we used the direct simple shear apparatus (DSS-H-12), developed by Bjerrum and Landva [18] at the Norwegian Geotechnical Institute (NGI) for the direct simple shear testing. The specimen was disturbed soil (referred to above), which was surrounded by a cylindrical wire-reinforced membrane to restrict the horizontal movement and circumference, with vertical pressure applied, during the consolidation stage (Fig. 2a). In this stage, the uniform distribution of stress and strain was applied to the soil specimen. In the subsequent loading stage, the horizontal shear force was applied to test the unrestricted horizontal movement. Also, in the loading stage, the undrained shear strength was measured by a constant volume test. The con-

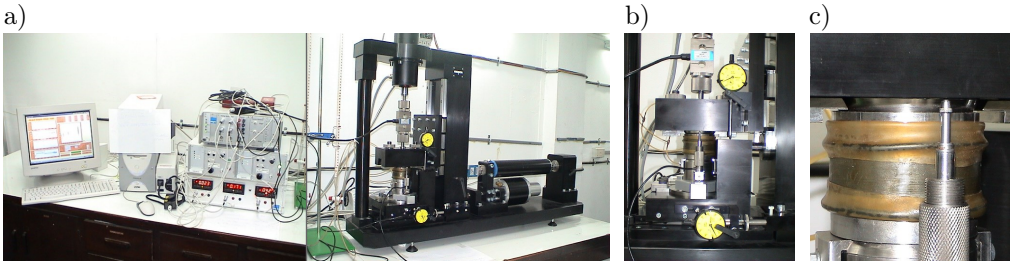

Fig. 2. Direct simple shear apparatus: a) DSS-H-12 direct simple shear apparatus, b) the specimens of the direct simple shear test, c) specimen in the apparatus.

stant volume test was programmed to maintain a constant sample height by the vertical load.

2.3. Sample preparation

A 20 mm soil sample was cut from the core in the 1 m Shelby tube, with a 35 cm^2 cross-section area and 67 mm diameter. This soil specimen was placed in a wire-reinforced membrane and installed in the direct simple shear apparatus (Figs 2b and 2c). The test specimen was prepared according to the step-by-step procedure listed in the user manuals of the DSS-H-12 apparatus [19]. An electronic linear variable differential transformer (LVDT), load cell and data logger were used to record the test data.

2.4. Undrained direct simple shear test procedure

Undrained direct simple shear tests were applied, first as monotonic tests and then cyclic tests. In the monotonic test procedure, the tests included a normally consolidated monotonic test (NCMT) and over-consolidation monotonic test (OCMT). The specimens were consolidated in K_0 state. Vertical axial stress was applied to the specimens, with fixed horizontal loading (Table 2). In the shearing stage, the horizontal shear force was applied to the specimen at the shearing rate of 5% shear strain per hour. The undrained shear strength was obtained by measuring the shear strain response, and the pore pressures were obtained by measuring the change in the vertical stress.

Table 2. Stress applied for consolidation.

Specimen name	OCR	σ'_{vm} [kPa]	σ'_{v0} [kPa]
NCMT-1	1.0	200	200.0
NCMT-2	1.0	300	300.0
NCMT-3	1.0	400	400.0
NCMT-4	1.0	500	500.0
OCMT-1	1.5	500	333.3
OCMT-2	2.0	500	250.0
OCMT-3	3.0	500	166.6
OCMT-4	4.0	500	125.0

Remark: OCR – $(\sigma'_{vm}/\sigma'_{vc})$, σ'_{vm} – maximum vertical effective stress, σ'_{vc}– effective vertical consolidation stress, and σ'_{v0} – overburden pressure.

In the cyclic test, normally consolidated cyclic test was performed on the soil specimen with K_0 – consolidation. A horizontal cyclic shear force under the

specified shear strain (γ), frequency and number of cycle (N) was applied to all specimens. The tests were conducted with a constant shear strain of 0.5% for the first 100 cycles of force, 1.5% for the next 100 cycles, and 3% for the last 100 cycles (Fig. 3). The speed of the cyclic shear force was varied in a sinusoidal fashion at frequencies of 0.1 Hz, 1 Hz and 5 Hz. The cyclic direct simple shear tests are summarized in Table 3.

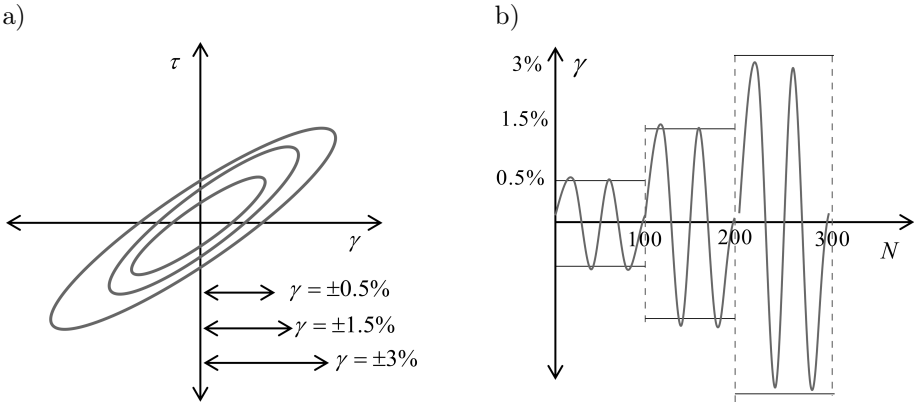

Fig. 3. Simulation of amplitude modulation of cyclic shear stress: a) shear stress vs. shear strain plot, b) shear strain vs. number of cycles.

Table 3. Summary of the cyclic direct simple shear tests.

Specimen	Frequency F [Hz]	σ'_{vm} [kPa]	The amplitude of cyclic shear strain		
			γ [%] (N = 1–100)	γ [%] (N = 100–200)	γ [%] (N = 200–300)
NCCT-1	0.1	200	±0.5	±1.5	±3
NCCT-2		300			
NCCT-3		400			
NCCT-4	1	200			
NCCT-5		300			
NCCT-6		400			
NCCT-7	5	200			
NCCT-8		300			
NCCT-9		400			

3. Results and discussion

3.1. Results and discussion of monotonic test

The normally consolidated and OC samples were sheared by a shear strain rate of 5 % per hour until a failure behavior occurred. The results are presented

by the normalized undrained shear strength (s_u/σ'_{vm}) with the maximum vertical effective stress at the end of consolidation (σ'_{vm}) versus shear strain (Fig. 4a). During the shear stage, the undrained shear strength increased as the shear strain increased, until the shear strain reached 20%. The failure behavior occurred when the undrained shear strength began to drop. In Fig. 4b, the normalized pore pressure ($\Delta u/\sigma'_{vm}$) was increased which rerated the shear strain increase. However, the pore pressures of OCR = 2, 3, and 4 decreased to negative values over the duration of the test. For OCR = 1.5, the pore pressure fluctuated.

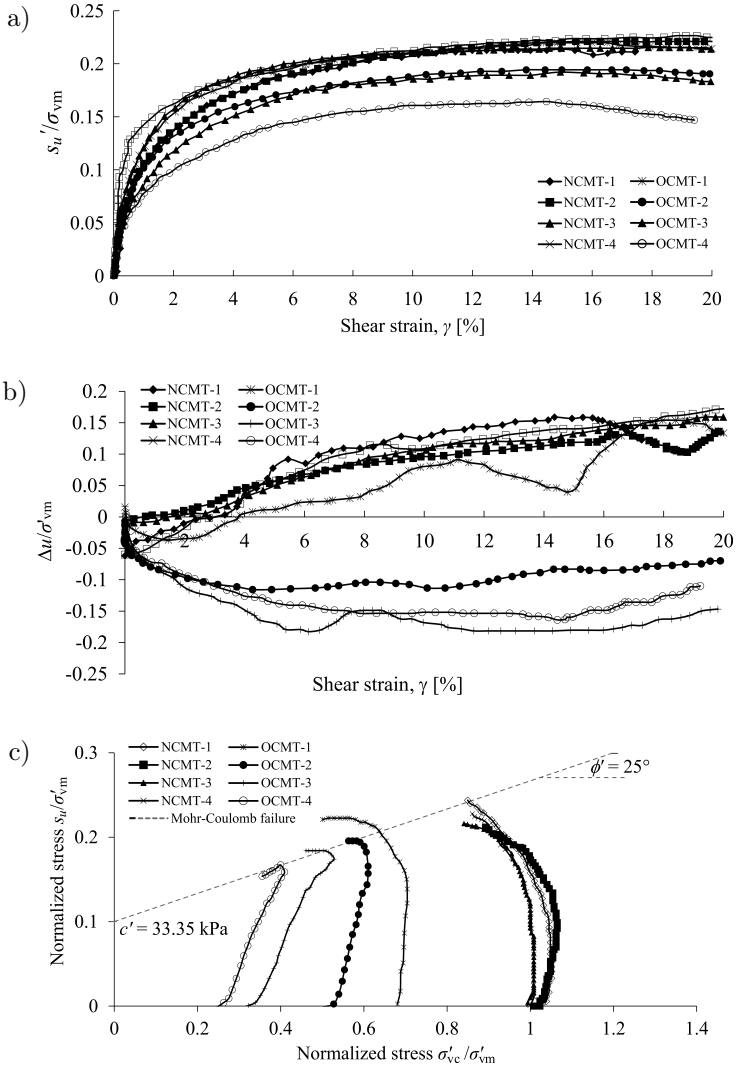

FIG. 4. Direct simple shear results: a) undrained shear strength, b) pore pressures, c) normalized stress path of Bangkok clay.

This behavior can be explained by atmospheric pressure changes which were the main contributor to pore pressure fluctuations for the periods when the soil water recharge and discharge were limited [20, 21]. Furthermore, the test results identified that the Mohr-Coulomb failure parameters were the angle of shearing resistance ($\phi' = 33.35°$) and the cohesion intercept ($c' = 25$ kPa) (Fig. 4c). The SHANSEP technique [19] was applied to analyze the strength parameters.

The new CK_0DSS SHANSEP parameters of Bangkok clay are proposed in Eq. (3.1), which was compared with the SHANSEP equation for the triaxial test results obtained by each [22]. The results showed that the CK_0DSS SHANSEP test is in a good correlation with the K_0 consolidated-undrained triaxial compression test (CK_0CU) and K_0 consolidated-undrained triaxial extension test (CK_0EU) (Fig. 5a)

$$\frac{s_{u(DSS)}}{\sigma'_{v0}} = s(\mathrm{OCR})^m, \tag{3.1}$$

where $s = 0.23$ and $m = 0.77$.

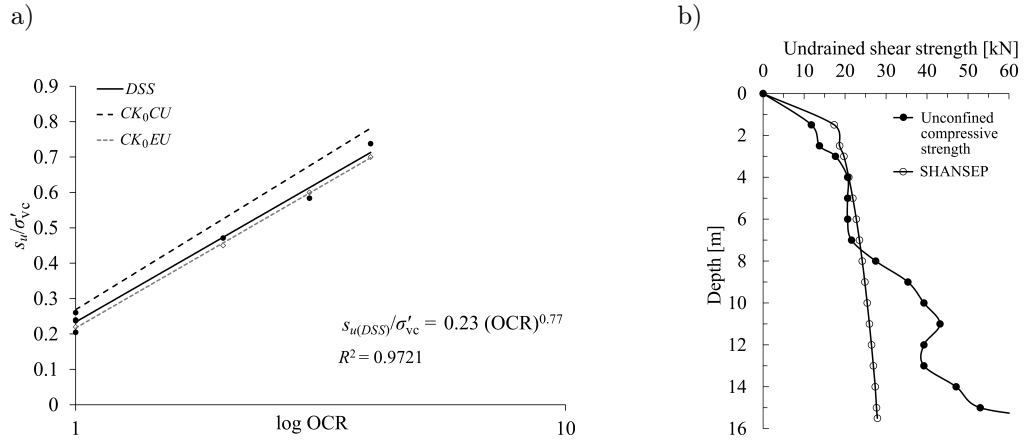

FIG. 5. SHANSEP curves for direct simple shear: a) compared with the triaxial test, b) compared with the unconfined compressive test.

The application of the CK_0DSS SHANSEP method was used to estimate the variation of the undrained shear strength with depth, and to compare the data from the bore log report against the unconfined compressive test (Q_u). The results from the CK_0DSS SHANSEP were consistent with the unconfined compressive strength results, at shallow soil depth (Fig. 5b). As well, the testing data were obtained from within the simple shear specimen, and the simple shear mode was used to estimate the skin friction of a pile [23].

3.2. Results and discussion of the cyclic tests

Each of the tests consisted of several stages of vertical effective consolidation stress. After primary consolidation, a horizontal cyclic shear force under the specified shear strain (γ), frequency, and number of cycles (N) was applied to all specimens. The tests were conducted with a constant shear strain of 0.5% for the first 100 cycles of force, 1.5% for the next 100 cycles of force, and 3% for the last 100 cycles of force. The speed of the cyclic shear force was varied in a sinusoidal fashion at frequencies of 0.1 Hz, 1 Hz, and 5 Hz. The shear stress, shear strain, and pore water pressure were obtained by the LVDT, load cell, and pore pressure transducer, which were linked to the data logger with computer monitoring.

The curves of shear stress (τ) and pore pressure, over a number of cycles, are plotted in Figs 6–14. These plots show that the pore pressure suddenly increased in the first phase of the cyclic test, and maintained that pressure until the test was finished. The undrained cyclic shear stress of NC clay consistently generates positive excess pore pressures. During the first 100 cycles of force, the pore pressures rapidly increased, then the values of pore pressures increased slowly during the last 100 cycles of force. When the cyclic shear strain in the second loading phase increased, the rate of build-up in excess pore pressures slowly increased as well. Under symmetric cyclic loadings, a hysteretic shear stress-shear strain relationship was exhibited on part c in Figs 6–14. The change in the cyclic shear stress was conducted by a corresponding change in the cyclic shear strain.

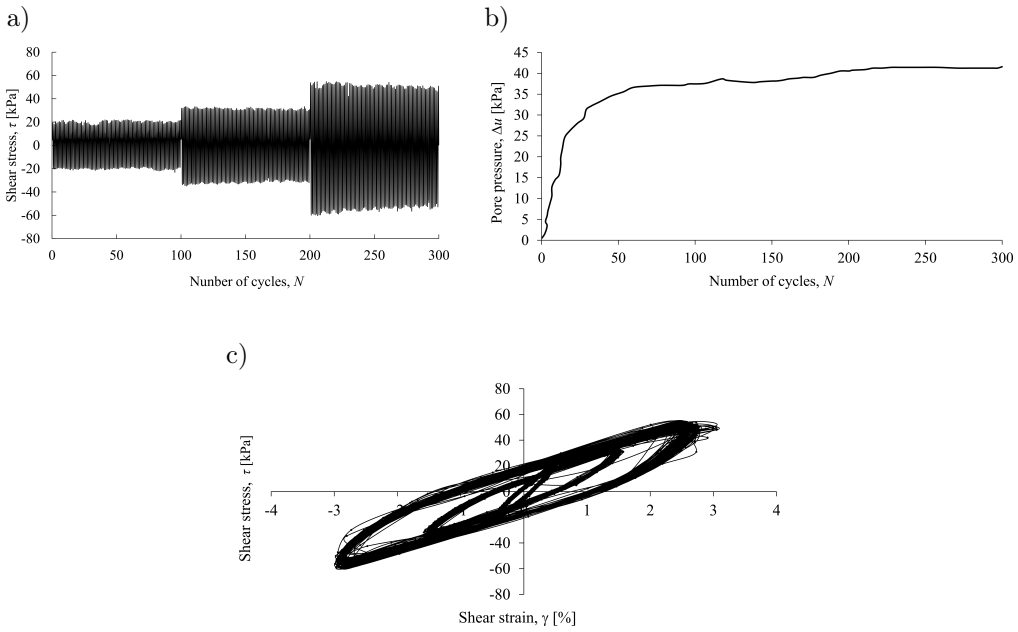

FIG. 6. NCCT-1 results: a) shear stress, b) pore pressure, c) hysteresis loop.

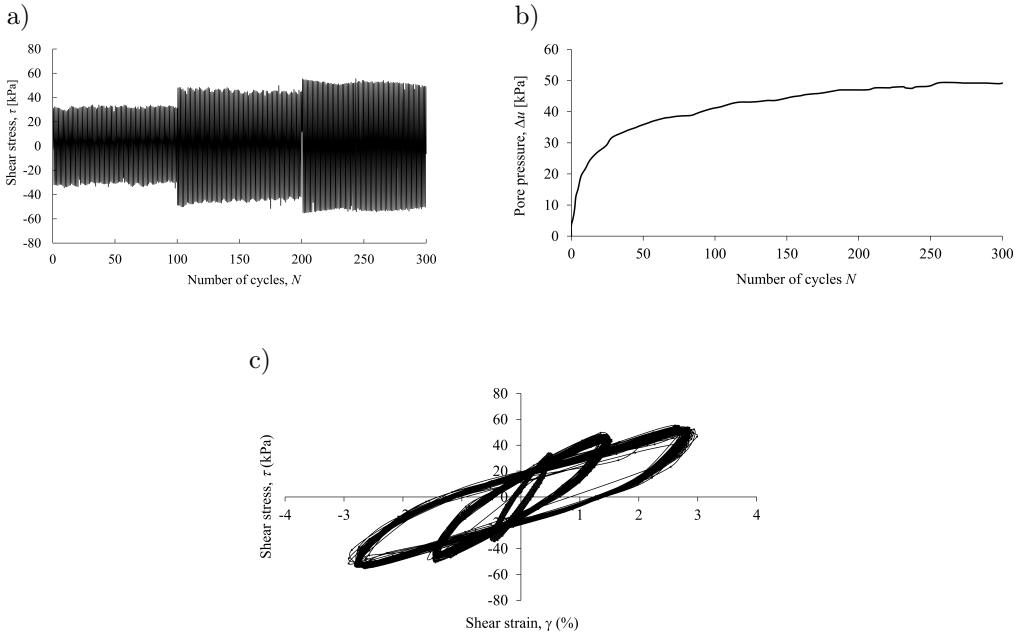

FIG. 7. NCCT-2 results: a) shear stress, b) pore pressure, c) hysteresis loop.

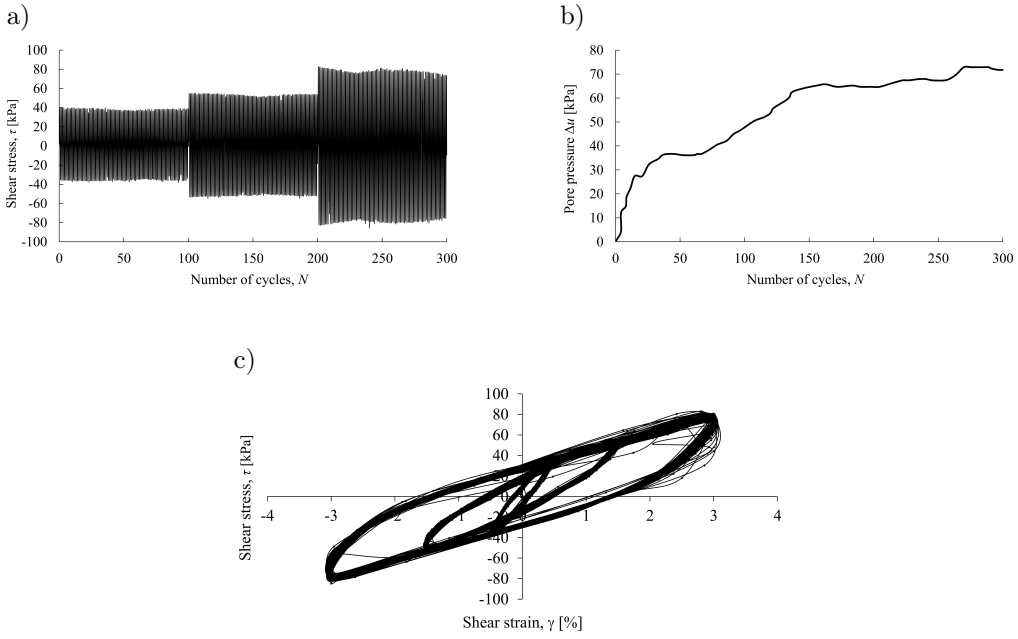

FIG. 8. NCCT-3 results: a) shear stress, b) pore pressure, c) hysteresis loop.

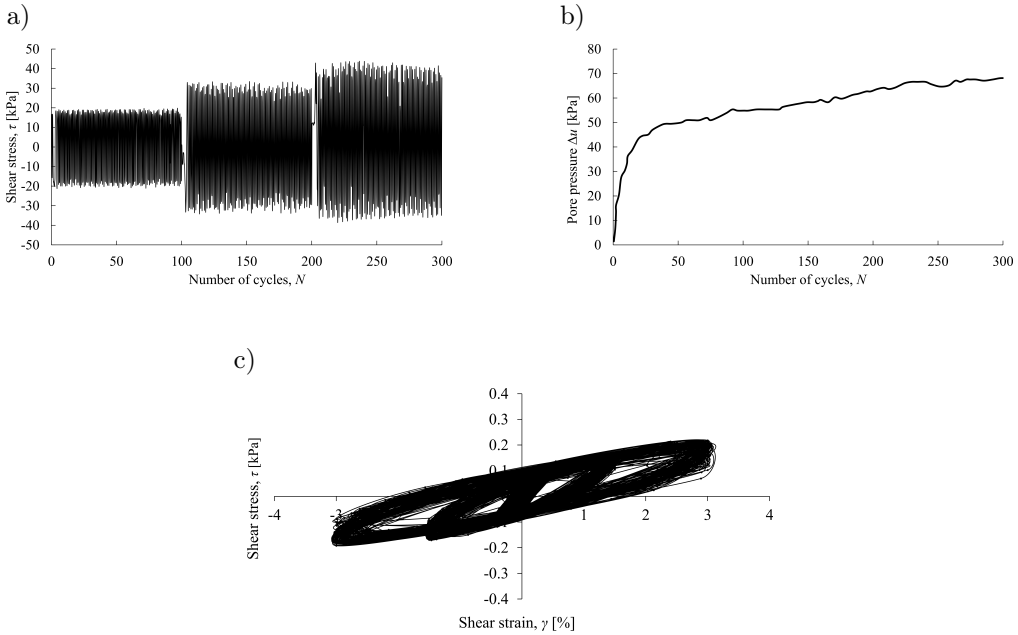

FIG. 9. NCCT-4 results: a) shear stress, b) pore pressure, c) hysteresis loop.

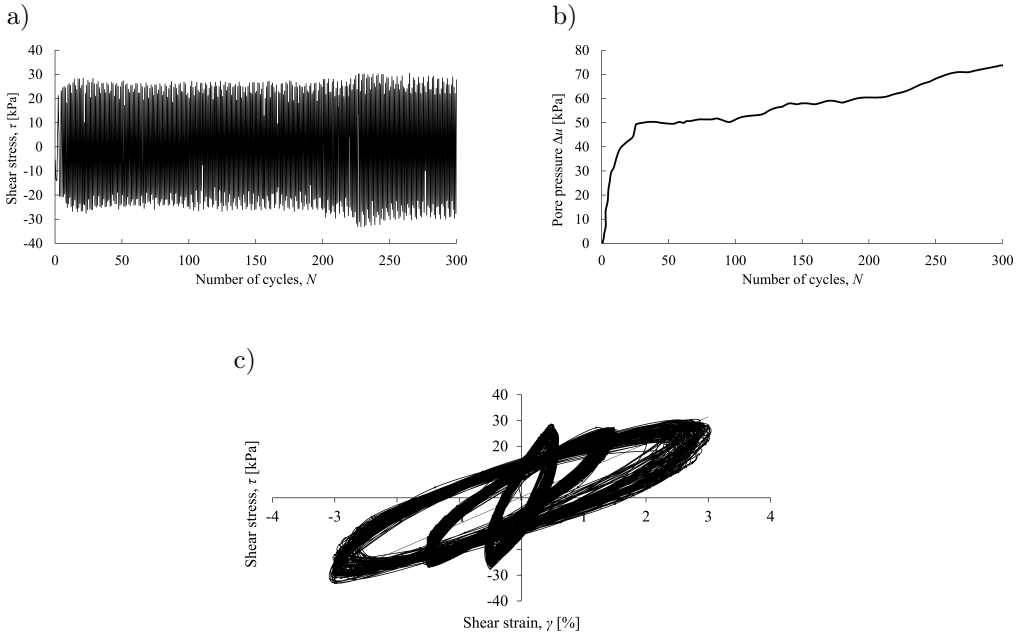

FIG. 10. NCCT-5 results: a) shear stress, b) pore pressure, c) hysteresis loop.

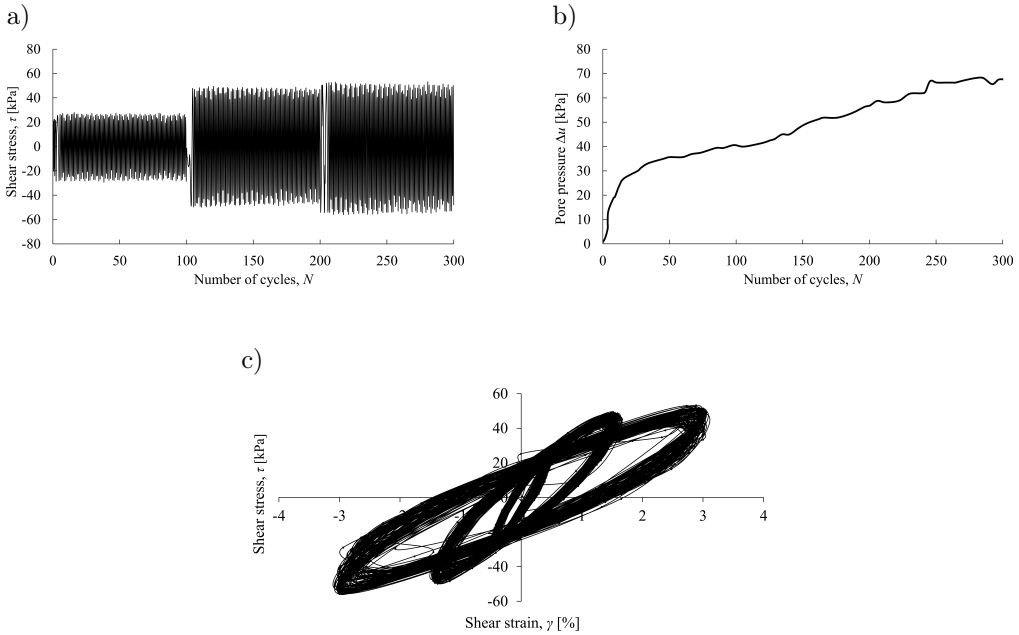

FIG. 11. NCCT-6 results: a) shear stress, b) pore pressure, c) hysteresis loop.

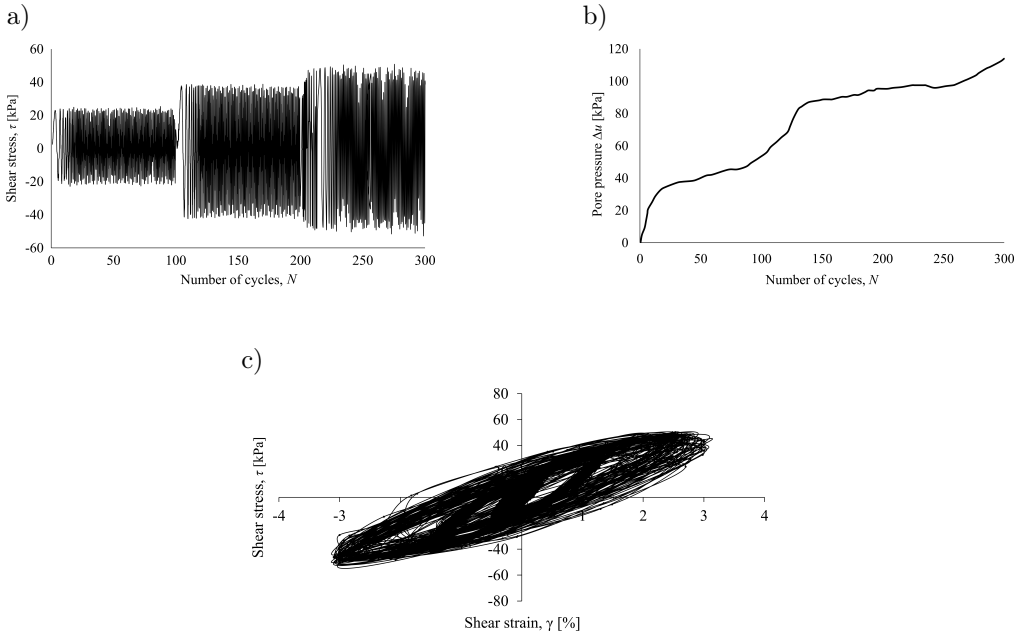

FIG. 12. NCCT-7 results: a) shear stress, b) pore pressure, c) hysteresis loop.

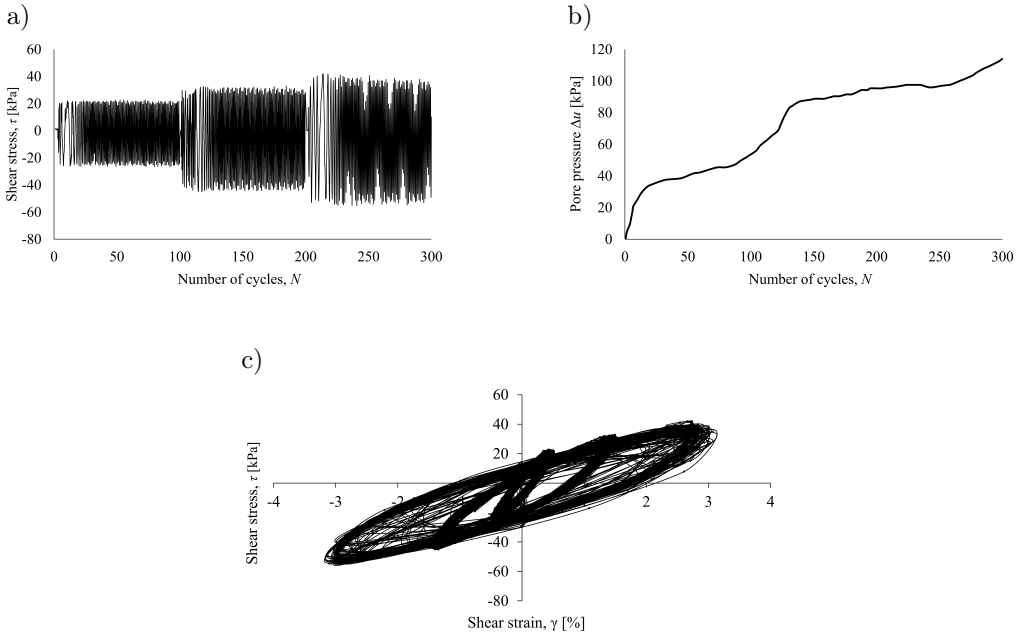

FIG. 13. NCCT-8 results: a) shear stress, b) pore pressure, c) hysteresis loop.

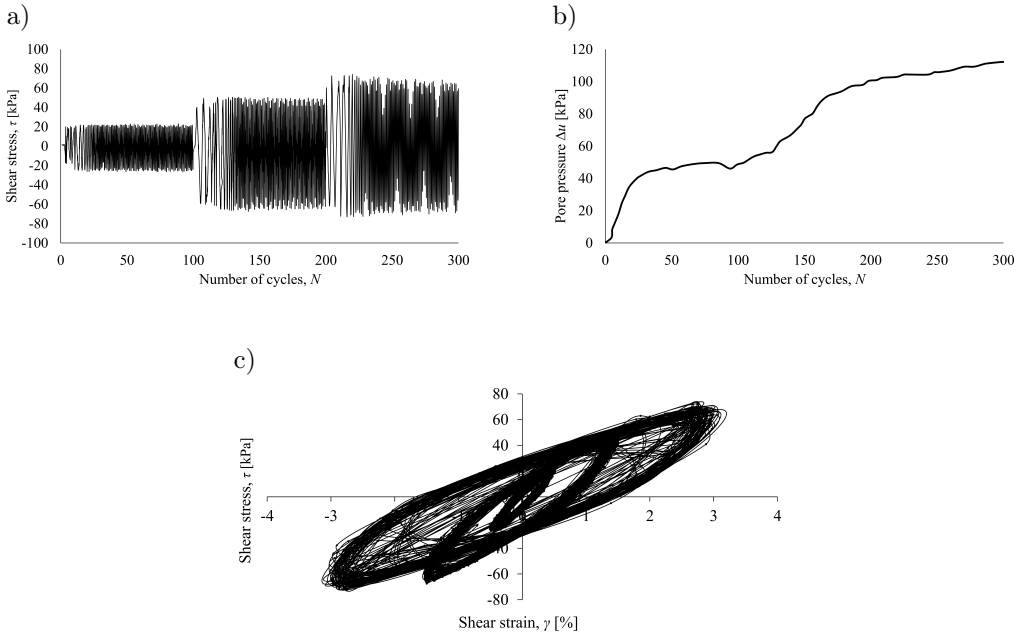

FIG. 14. NCCT-9 results: a) shear stress, b) pore pressure, c) hysteresis loop.

The parameters influencing the inclination and the breadth of the hysteresis loop are shear modulus (G) and damping (D). The tangent shear modulus ($G_{\tan}$) and secant shear modulus ($G_{\sec}$) are generally used to describe the variations of soil stiffness (Fig. 15a). However, the tangent shear modulus changed along the path of the hysteresis loop, and became a high trust value at low shear strain amplitudes, while the secant stiffness varied as the number of cyclic loads increased (Fig. 15b). Thus, the equivalent secant shear modulus (G_{eq}) is an effective method for calculating the collective results. Additionally, the normalized equivalent secant shear modulus by the maximum shear modulus ($G_{\mathrm{eq}}/G_{\max}$) is a well-known tool for defining the small-strain stiffness characteristics of soils and earthquake site response analyses [24, 25].

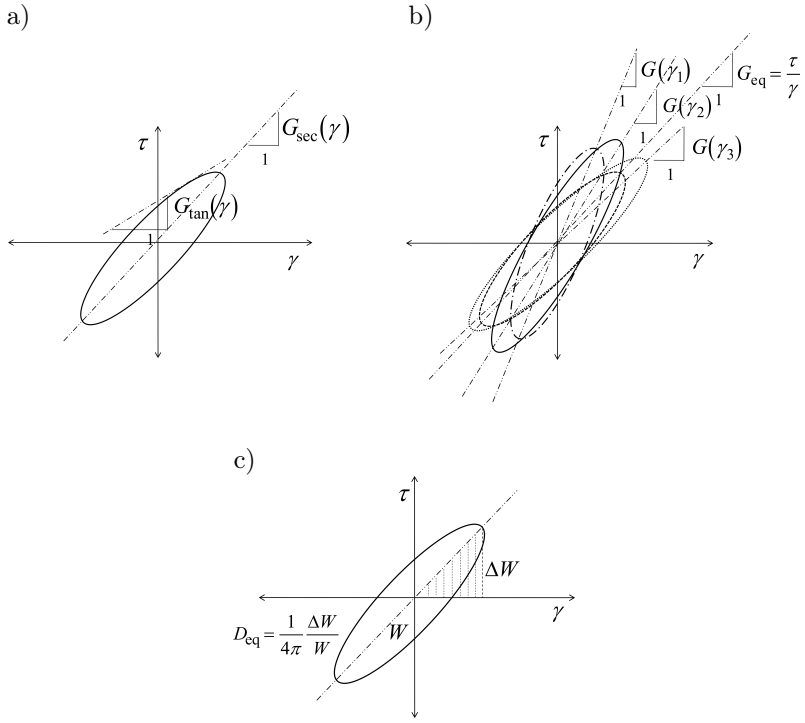

FIG. 15. Parameters significant for the cyclic behavior of soils: a) tangent shear modulus and secant shear modulus in a hysteresis loop, b) definition of average shear modulus, c) definition of average damping ratio.

In the present research, the equivalent secant shear modulus, the maximum shear modulus ($G_{\max}$), and the equivalent damping ratio (D_{eq}) were calculated by Eqs (3.2)–(3.4). The equivalent secant shear modulus and damping ratio of Bangkok clay are shown in Fig. 16

$$G_{\mathrm{eq}} = \frac{\tau}{\gamma}, \tag{3.2}$$

$$G_{\max} = 625 \frac{p_a^{1-n} \left(\sigma_m^{'}\right)^n}{(0.3 + 0.7e^2)} (\mathrm{OCR})^k, \tag{3.3}$$

$$D_{\mathrm{eq}} = \frac{1}{4\pi} \frac{\Delta W}{W}, \tag{3.4}$$

where ΔW and W are an area of hysteresis loop (Fig. 15c), p_a is the atmosphere pressure (100 kPa), e is a void ratio, n is the stress component (usually taken as 0.5), σ'_m is the mean principal effective stress ($(\sigma'_v + \sigma'_h)/2$ or $(\sigma'_v + K_0\sigma'_v)/2$, $K_0 = 1 - \sin\phi'$), and k is an over-consolidation ratio exponent as shown in Table 4.

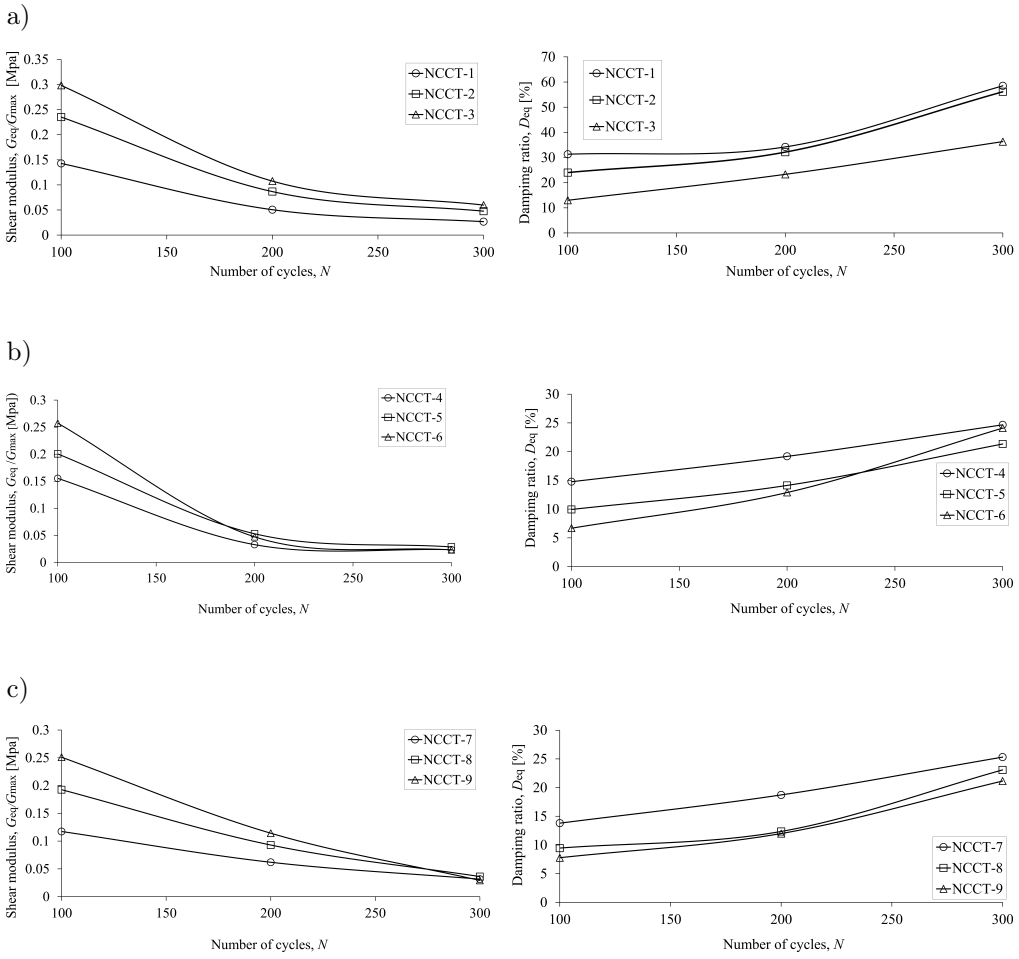

FIG. 16. The curve of normalized shear modulus and damping ratio: a) the results of NCCT-1, NCCT-2 and NCCT-3, b) the results of NCCT-4, NCCT-5 and NCCT-6, c) the results of NCCT-7, NCCT-8 and NCCT-9.

Table 4. Over-consolidation ratio exponent [26].

Plastic Index, PI [%]	k
0	0.00
20	0.18
40	0.30
60	0.41
80	0.48
≥ 100	0.50

The curve of the results shows that the normalized shear modulus increased with increased vertical effective stress, but the damping ratio was decreased. The reason for this phenomenon in the results is that the soil particles pack together more tightly when the vertical effective stress is applied. This results in the soil stiffness properties becoming much stronger. As the shear strain amplitudes increased, the normalized shear modulus decreased whereas the damping ratio increased. Because the strength of soils to resist deformation has reduced, more energy is released, creating high deformation. When the number of loading cycles increases, the normalized shear modulus decreases, with a related increase in pore pressure. Furthermore, the loading frequency was extremely affected by the pore pressure increase, as the soil particle cannot always release the pore pressure with higher load frequency. Finally, the cyclic shear stress (τ), pore water pressure (Δu), shear modulus (G_{avg}) and damping ratio (D_{avg}) were the fundamental parameters for dynamic foundation design.

4. Conclusion

The monotonic and cyclic responses of Bangkok clay have been presented in this research. The specimens were sampled from cores drilled to 15.5 m depth and contained in a 1 m Shelby tube from an area near central Bangkok. Four normally consolidated and four over-consolidation samples were tested and analyzed by the SHANSEP method, and a new SHANSEP equation was proposed. The SHANSEP parameters were obtained by CK_0DSS tests with values $s = 0.23$ and $m = 0.77$. The results from the new CK_0DSS SHANSEP equation were in good correlation with CK_0CU and CK_0EU. The undrained shear strength prediction by the CK_0DSS SHANSEP equation was well correlated with the unconfined compressive strength from the bore log report. The parameters based on the Mohr-Coulomb failure envelope were $c' = 25^\circ$ and $\phi' = 33.35$ kPa. The cyclic simple shear tests were conducted at different frequencies of 0.1, 1, and 5 Hz, and the vertical stress was varied from 200, 300, and 400 kPa. The test procedures were controlled at $\pm 0.5\%$ for the first 100 cycles, then the shear strain amplitude

was increased to ±1.5% for the next 100 cycles and then increased up to ±3% for the last 100 cycles. According to the results, the vertical effective stress, the shear strain amplitudes and number of loading cycles were the major factors contributing to the variations in the shear modulus and damping ratio values.

Conflict of interest

The authors wish to confirm that there are no known conflicts of interest associated with this publication.

Acknowledgment

The authors greatly appreciate Mr. Piroj Anatasetakul for his assistance with the adjustment of the cyclic control system for direct simple shear apparatus. We acknowledge the contribution of Mr. Roy I. Morien from the Naresuan University Graduate School for his assistance in editing the English expression and grammar in this paper.

References

1. Roscoe K.H., *The influence of strains in soil mechanics*, Geotechnique, **20**(2): 129–170, 1970.
2. Finn L., Pickering W.D., Bransby P.L., *Sand liquefaction in triaxial and simple shear tests*, Journal of the Soil Mechanics and Foundations Division, **97**(4): 639–659, 1971.
3. Lucks A., Christian J., Brandow G., Hoeg K., *Stress conditions in NGI simple shear test*, Journal of the Soil Mechanics and Foundations Division, **98**(1): 155–160, 1972.
4. Prevost J., Hoeg K., *Reanalysis of simple shear soil testing*, Canadian Geotechnical Journal, **13**(4): 418–429, 1976.
5. Shen C.K., Sadigh K., Herrmann L.R., *An analysis of NGI simple shear apparatus for cyclic load testing*, Dynamic Geotechnical Testing, **STP 654**: 148–162, 1978.
6. Andersen K., Pool J., Brown S., Rosenbrand W., *Cyclic and static laboratory tests on Drammen clay*, Journal of the Geotechnical Engineering Division, **106**(5): 499–529, 1980.
7. Seed H.B., Chan C.K., *Clay strength under earthquake loading conditions*, Journal of the Soil Mechanics and Foundations Division, **92**(SM2): 53–78, 1966.
8. Yasuhara K., Hirao K., Hyde L., *Effects of cyclic loading on undrained strength and compressibility of clay*, Soils and Foundations, **3291**: 100–116, 1992.
9. Zhou J., Gong X., *Strain degradation of saturated clay under cyclic loading*, Canadian Geotechnical Journal, **38**(1): 208–212, 2001.
10. Ni J., Indraratna B., Geng X.Y., Carter J.P., Chen Y.L., *Model of soft soils under cyclic loading*, International Journal of Geomechanics, **15**(4): 04014067, 2014.
11. Indraratna B., Sun Y., Nimbalkar S., *Laboratory assessment of the role of particle size distribution on the deformation and degradation of ballast under cyclic loading*, Journal of Geotechnical and Geoenvironmental Engineering, **142**(7): 04016016, 2016.

12. Thian S.Y., Lee C.Y., *Cyclic stress-controlled tests on offshore clay*, Journal of Rock Mechanics and Geotechnical Engineering, **9**(2): 376–381, 2017.

13. Teerachaikulpanich N., Phupat V., *Geological and geotechnical engineering properties of Bangkok clay*, Proceedings of the 38th Japan National Conference on Geotechnical Engineering, 2005.

14. Casagrade A., Wilson S.D., *Effect of rate of loading on the strength of clay and shales at constant water content*, Geotechnique, **2**(3): 251–263, 1951.

15. Hardin B.O., Black W.L., *Vibration modulus of normally consolidated clay*, Journal of Soil Mechanics and Foundation Division ASCE, **94**(SM2): 353–369, 1968.

16. Pailoplee S., Charusiri P., *Seismic hazards in Thailand: a compilation and updated probabilistic analysis*, Earth, Planets and Space, 68–98, 2016.

17. Ladd C.C., Foott R., *New design procedure for stability of soft clays*, Journal of the Geotechnical Engineering Division, **100**(7): 763–786, 1974.

18. Bjerrum L., Landva A., *Direct simple shear tests on a Norwegian quick clay*, Géotechnique, **16**(1): 1–22, 1966.

19. GEONOR, *Instructions for use of direct simple shear apparatus*, GEONOR Inc., Østerås, Norway, 1999.

20. Hsieh P.A., Bredehoeft J.D., Farr J.M., *Determination of aquifer transmissivity from Earth tide analysis*, Water Resources Research, **23**(10): 1824–1832, 1987.

21. Rojstaczer S., *Intermediate period response of water levels in wells to crustal strain: sensitivity and noise level*, Journal of Geophysical Research: Solid Earth, **93**(B11): 13619–13634, 1988.

22. Sambhandharaksa S., *Stress-strain-strength anisotropy of varved clays*, Doctoral thesis, Massachusetts Institute of Technology, Boston, U.S.A., 1977.

23. Yasufuku N., Ochiai H., *Skin friction of non-displacement piles related to simple shear mode with large strain state friction angle*, Soils and Foundations, **46**(4): 537–544, 2006.

24. Szajna W.S., *Evaluation of the state of sandy soils on a sinkhole area with the use of noninvasive (MASW) and invasive (SDMT) tests*, Engineering Transactions, **63**(1): 109–131, 2015.

25. Tong L.Y, Che H.B., Zhang M.F., Pan H.S., *Determination of shear wave velocity of Yangtze Delta sediments using seismic piezocone tests*, Transportation Geotechnics, **14**: 29–40, 2018.

26. Hardin B.O., *The nature of stress-strain behaviour for soils*, Proceedings of Earthquake Engineering and Soil Dynamics ASCE, pp. 19–21, 1987.

Received July 28, 2018; accepted version January 28, 2019.
